Journal of Materials Chemistry

Cite this: J. Mater. Chem., 2011, 21, 3391

www.rsc.org/materials

PAPER

The effects of thionyl chloride on the properties of graphene and graphene–carbon nanotube composites

Jonathan K. Wassei,†[a] Kitty C. Cha,†[b] Vincent C. Tung,[b] Yang Yang*[b] and Richard B. Kaner*[ab]

Received 2nd September 2010, Accepted 6th January 2011
DOI: 10.1039/c0jm02910f

Anionic dopants have been used to reduce the overall sheet resistance of carbon nanotube and graphene films for transparent conductor applications. These enhanced electronic properties are attributed to an increased number of p-type charge carriers. While there have been many reports of its use, there is little reported insight into the chemical interactions of a commonly used dopant, thionyl chloride ($SOCl_2$), with pristine graphene and its chemically converted derivatives. Here, we explore the effects of thionyl chloride on the physical and chemical properties of graphene and hybrid graphene–carbon nanotube films, focusing on how the changes in conductivity correlate to the morphology of chemically converted graphene and carbon nanotube composites.

Introduction

Graphene has been a highly sought after material since its first reported isolation in 2004.[1] In recent years, there have been several reports discussing its possible uses as a transparent conductor in touch screens, solid-state lighting and solar cells.[2–6] As most graphenes produced by CVD and chemical reduction processes have yet to record conductivities high enough for electrode applications, doping of these materials has been studied.[7–9] Doping processes of CVD graphene with nitric acid, nitromethane and $AuCl_3$ show characteristics of p-doping,[8–10] while polyvinyl alcohol is reported to n-dope mechanically exfoliated graphene.[11] Doping can reduce the resistance of graphene films to a few hundreds of Ω, bringing it to the range of indium tin oxide. Modification of carbon nanotubes has been carried out using a number of species in the vapour and liquid phases. Thionyl chloride ($SOCl_2$) is a commonly used solvent and inorganic acid known for dehydrating and chlorinating oxygen containing hydrocarbons. Similar effects have been observed in nanotubes exposed to strong inorganic acids such as nitric and sulfuric acids, but these effects are believed to be due to oxidation and removal of surfactant groups.[12] Thionyl chloride is capable of comprehensively modifying the basal planes and open ends of graphitic materials, creating platforms for attachment of a variety of functionalities.[13,14] Previous work has shown that the conductivity of single-walled carbon nanotubes increases upon treatment with $SOCl_2$.[3–5,14] The modification process involves simple immersion either in liquid or vapour phase $SOCl_2$, so the mechanism behind their increased conductivity warrants further analysis. Similarly, their structural similarities with carbon nanotubes make it logical that the graphene and composites of graphene and carbon nanotubes (G–CNT) would be affected by this chemical treatment in an analogous manner. While there have been reports on dopant- or solvent-induced changes in the electronic properties of graphitic materials, there has been a lack of conclusive evidence to explain the improvement in conductivity in chemically converted graphene and graphene–CNT nanocomposites treated with $SOCl_2$. In this study, we explore the effects of thionyl chloride on the physical and chemical properties of pristine graphene and examine the changes in the structure and morphology of G–CNT nanocomposites that lead to improvements in their transparent conducting properties.

Experimental section

Sample preparation

Chemically Converted Graphene (CCG) and Graphene–carbon nanotube (G–CNT) nanocomposite films were prepared using previously reported procedures.[2] GO was obtained *via* oxidation of graphite using Hummers' method, followed by filtration to remove water. The GO paper was then dispersed and reduced in anhydrous hydrazine without surfactants. This dispersion was purified after being mixed for one week to insure complete reaction. The CCG dispersion was then centrifuged at 1500 rpm for 60 minutes and the top 40 μl of the supernatant was collected and diluted with 60 μl of fresh hydrazine to reliably disperse the single sheets.[2,17] Similarly, SWCNTs were weighed out and dispersed into anhydrous hydrazine for one week. The resulting dispersion was centrifuged at 2000 rpm for 60 minutes and the

[a]*Department of Chemistry and Biochemistry and the California NanoSystems Institute, University of California Los Angeles, Los Angeles, CA, USA. E-mail: kaner@chem.ucla.edu; Tel: +1 310 825 5346*
[b]*Department of Materials Science and Engineering and the California NanoSystems Institute, University of California Los Angeles, Los Angeles, CA, USA. E-mail: kaner@chem.ucla.edu; Tel: +1 310 825 5346; yangy@ucla.edu; +1 310 825 4052*
† These authors contributed equally.

top 40 μl was collected and diluted with fresh anhydrous hydrazine. These two dispersions were then mixed in a ratio of 1 part CCG to 5 parts CNTs. Films were then deposited from surfactant-free dispersions in hydrazine onto a myriad of substrates by spin-coating. A mild annealing process, at 110 °C, was applied to ensure adequate removal of the solvent. Additional studies on graphene were performed on sheets of mechanically exfoliated graphene, or pristine graphene, which were transferred onto silicon substrates with a thermally grown 300 nm silicon oxide.

Thionyl chloride doping

Vapour treatments were performed in glass Petri dishes. Substrates with dried CCG, G–CNT composites and pristine graphene were placed into these vapour treatment chambers and ~1 mL of liquid $SOCl_2$ was dispensed into the dishes and around the samples, with care taken to avoid direct contact. We find that extended immersion in thionyl chloride results in complete delamination from the substrate. The dishes were covered and allowed to saturate with vapour at 135 °C for at least 15 minutes, or until the vapour had dissipated.

Characterization

Raman spectra were obtained using a Renishaw 1000, with a 50× objective lens at an excitation wavelength of 514 nm. The peaks were fit using the Renishaw software to confirm the location of the Raman peaks. X-Ray photoemission spectroscopy (XPS) was carried out in an Omicron Nanotechnology system with a base pressure of 2×10^{-10} Torr with Al Kα radiation (1486.6 eV) as the excitation source. The sheets of chemically converted graphene were scanned with a Veeco Dimension 5000 atomic force microscope before and after $SOCl_2$ treatment to obtain high resolution images. Absorbance and transmittance measurements were carried out using a Cary 50 UV-visible spectrophotometer under ambient condition. Scanning electron micrographs (SEM) of the graphene and G–CNT composites were obtained on a JEOL 6700 SEM. Additionally, Energy-Dispersive X-ray spectra were obtained using an EDAX Genesis detector attached to the SEM.

Results and discussion

Raman spectroscopy

Raman spectroscopy is a versatile and non-destructive characterization technique for obtaining information on the quality of many poly-aromatic hydrocarbons. The assignment of the D and G peaks, and their overtones, is now a straightforward process that has been discussed at great length.[13–15] The Raman spectra of all carbon materials are dominated by sp^2 vibrations, since visible excitations resonate with π states, while sp^3 sites can only be activated upon UV excitation.[14,15] The G peak, which resides at ~1560 cm^{-1}, is a result of bond stretching from all pairs of sp^2 atoms in both rings and chains.[18–20]

The G-band in graphitic materials typically exhibits a substantial upshift for electron-acceptor dopants (*e.g.* bromine, iodine and nitric acid), while displaying a downshift for electron-donor (*e.g.* potassium) dopants.[21] Upon exposure to thionyl chloride vapour, electrons originally residing on the graphitic framework are pulled toward the more electronegative atoms, leading to charge redistribution.

Raman spectra were obtained for chemically converted graphene, mechanically exfoliated graphene (pG) and CCG–CNT

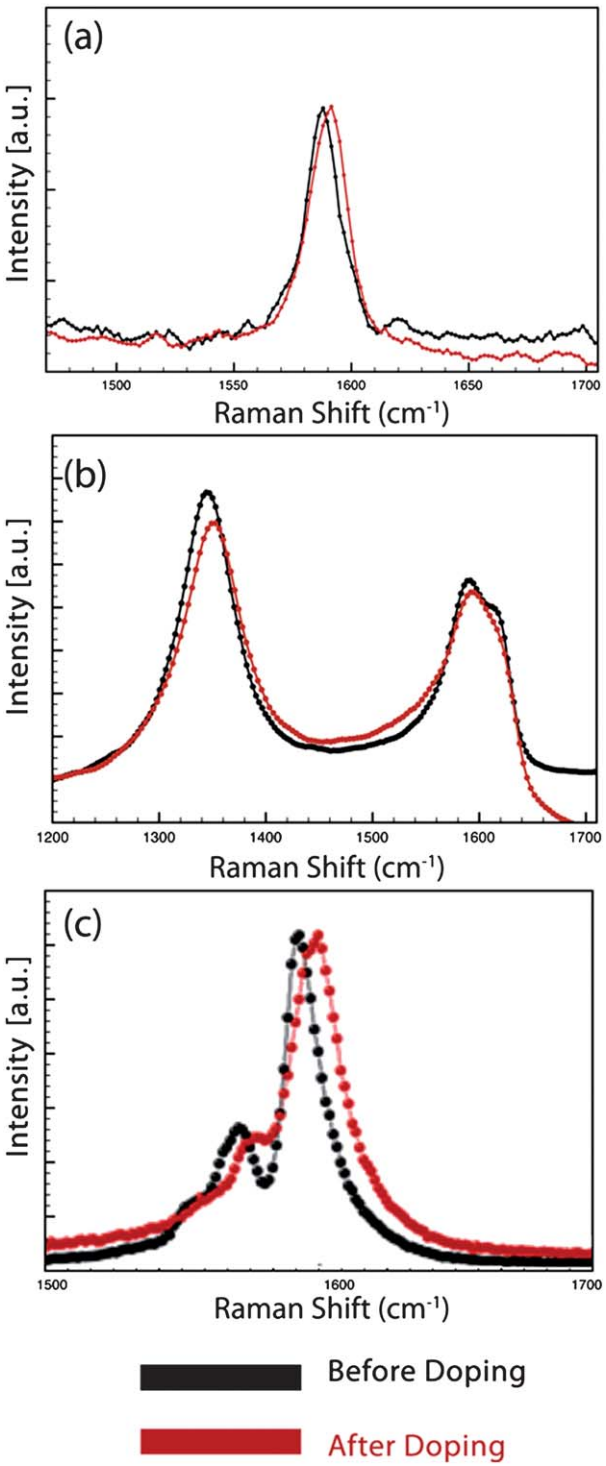

Fig. 1 An upshift in the Raman spectrum for the G peak is observed after fifteen minutes of thionyl chloride exposure. (a) A pristine graphene flake red shifts by 5.2 cm^{-1}; (b) a chemically converted graphene flake shifts by 4.8 cm^{-1}; and (c) a CCG–CNT hybrid film red shifts by 8.1 cm^{-1}.

composites, before and after 15 minutes of thionyl chloride exposure (Fig. 1). The full width at half maximum (fwhm) for the 2D mode of our pristine graphene was measured to be 33 cm^{-1}, indicating a single layer was being used for this experiment. Blue-shifts in CCG (Fig. 1a) from 1595.9 to 1601.1 cm^{-1} (~5.2 cm^{-1}), pristine graphene (Fig. 1b) from 1587.7 to 1592.5cm^{-1} (~4.8 cm^{-1}) and G–CNT (Fig. 1c) from 1592.1 to 1600.2 cm^{-1} (~8.1 cm^{-1}) are observed, which signify electron transfer from the graphitic materials to the dopant (Fig. 1 and Table 1). The shape of the G band can also be used to understand the changes in the in-plane force constant and determine if a graphene flake has been intercalated.[22] As shown in Fig. 1a–c, no splitting of the G peak is observed, indicting that this anionic interaction does not form an intercalated compound. This is important in understanding the role of the anionic dopant in the graphene system. The physical adsorption of anions is a similar effect to that of other halogen dopants such as bromine or iodine, whereas nitric acid and diazonium are believed to intercalate into the graphitic layers.[7] The shape of the G peak in the G–CNT system (Fig. 1c) is an exception to the splitting since its shape is a result of combining mostly semiconducting carbon nanotubes with CCG.

Chemical bonding of thionyl chloride to the graphitic structures

To gain insight into the effect of thionyl chloride on graphene we used XPS and EDX to elucidate bonding information on graphene, CCG and G–CNT thin films. The nature of the chemical modification to the graphitic structures was determined by XPS analysis. Spectra were collected for pristine graphene, CCG and G–CNT that were deposited onto silicon substrates with a 20 nm gold layer added on top to avoid charging effects. It has been shown that the pristine SWCNT forms many C–S bonds and some C–Cl bonds when exposed to liquid $SOCl_2$ at elevated temperatures,[14] so similar doping interactions with pristine graphene were expected. Full core level spectra for all three samples were collected and evidence for C 1s and Cl 2p peaks were found,[16] but S 2p, which was observed in previous experiments with CNTs, was not found. These results suggest that either the curvature and the absence of carboxylic acid groups on the CNT allows for molecular interaction of the $SOCl_2$ with the carbon and resulting C–S bonds or the $SOCl_2$ fully decomposes in the vapour phase. In all instances the XPS show the same C 1s (for sp^2 C) and Cl 2p (C–Cl) binding energies. Fig. 2a and b presents the results for CCG flakes before and after treatment. Our results indicate that C–Cl interactions form from the doping process, which leads to the overall enhancement in the electronic transport.

The C 1s peak at 284.4 eV for sp^2 carbon shifts by 0.5 eV to a lower binding energy (283.9 eV) after the vapour treatment, indicating that the sp^2 pi system has been affected. The Cl 2p core level spectrum shows two nonequivalent chlorine sites from the 3/2 and 1/2 levels, which are separated by 1.4 eV due to spin–orbit coupling. The more intense peak at ~200.2 eV is a result of Cl participating in C–Cl covalent bonding, while the less intense peak at ~198.8 eV is a result of Cl^- ionic bonds with the carbon on the surface. This is significant as it shows that the graphitic surfaces in the pG, CCG and G–CNT are modified by interactions with the Cl in the thionyl chloride, instead of the S in unfunctionalized CNTs.

Table 1 Optical and electronic properties of G–CNT composite films before and after thionyl chloride treatment

G–CNT sample	Optical transmittance	Sheet resistance	Raman shift
Untreated	82%	425 Ω □$^{-1}$	1592 cm^{-1}
$SOCl_2$ doped	82%	103 Ω □$^{-1}$	1600 cm^{-1}

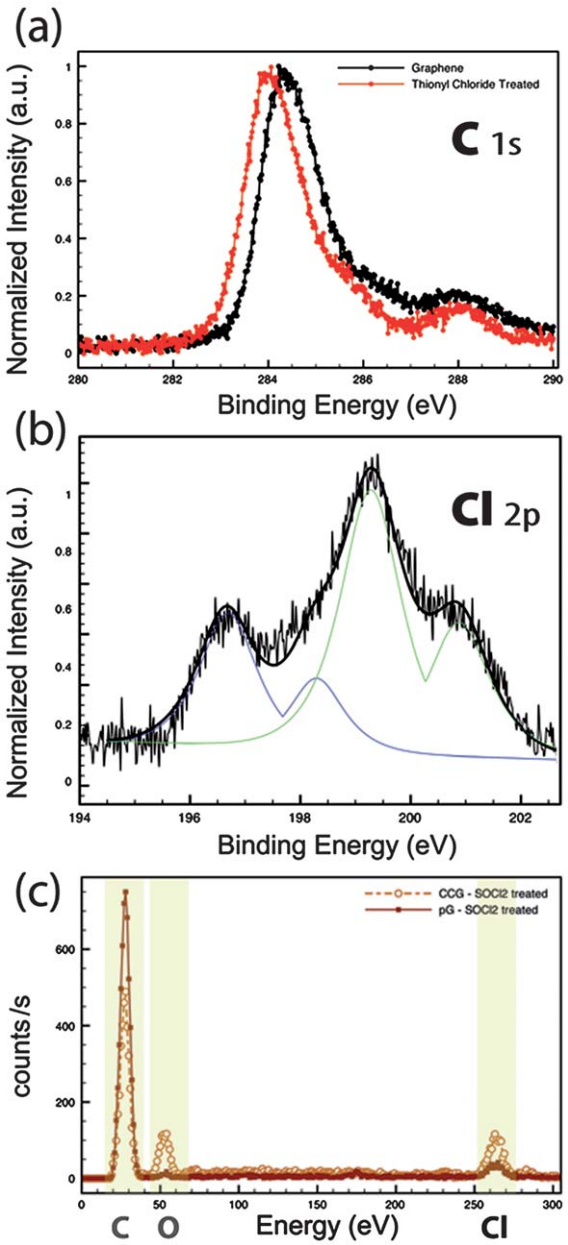

Fig. 2 X-ray photoemission spectra of thionyl chloride treated graphene materials were taken to probe their chemical bonding: (a) C 1s and (b) Cl 2p of graphene. The chemical composition of the materials was probed, after treatment, using energy dispersive X-ray (EDX) spectroscopy for (c) both mechanically exfoliated pristine graphene (pG) and chemically converted graphene (CCG) to verify the presence of chlorine.

To confirm the chemical composition of the modified graphitic species, EDX spectra were collected on both pristine and chemically converted graphene species. Fig. 2c verifies that only chlorine, carbon and oxygen (in the case of CCG) on the graphene and G–CNT post-$SOCl_2$ treatment are present.

Morphological changes to G–CNT composites

The changes in chemical structure can be correlated to the morphology of the composites using scanning electron microscopy (SEM). Thicker multilayer composites were analyzed, and the micrographs show that the treatment promotes not only aggregation and cross-linking among nanotube bundles, but also between the nanotubes and the graphene sheets. These results show that chlorine, not sulfur-bound thionyl chloride, must be responsible for this morphological change. SEM images (Fig. 3) suggest that the chemical modification with $SOCl_2$ facilitates stronger interactions between the carbon nanotubes and graphene (Fig. 3a,b). The images of graphene layers alone (Fig. 3c,d) show that the thionyl chloride treatment also promotes aggregation between layers and the incorporation of carbon nanotubes clearly provides an additional pathway for 3-dimensional interactions.

The bundling, coupled with the lack of G peak splitting from the Raman spectra suggests that chlorine anions, from thionyl chloride, also act as adsorbants rather than intercalants. AFM images further suggest that instead of folding along preferred crystallographic planes, the graphene flakes slightly wrinkle, and in the case of CCG, they also rip (Fig. 3e,f). No significant change in step height was measured on surveying the surface of the CCG with an atomic force microscope tip, implying that either these anions are not strong enough to induce folding or the concentration of the adsorbed vapour was insufficient to induce the type of folding previously seen with sulfate anions.[22]

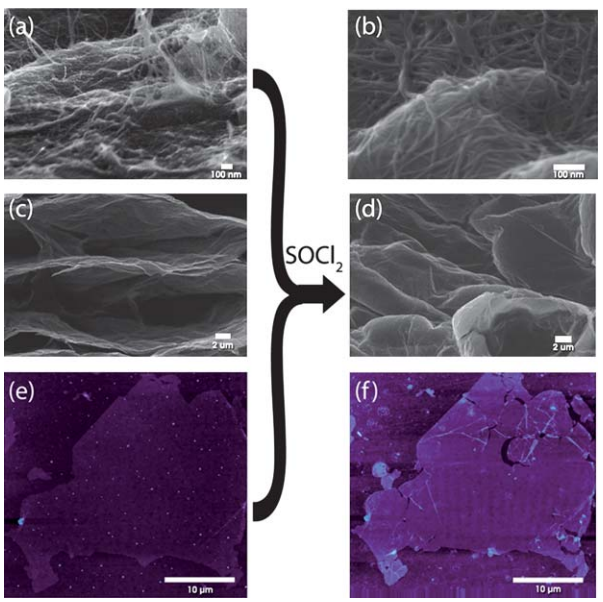

Fig. 3 Representative scanning electron micrographs (SEM) of graphene–CNTs nanocomposites and CCG and an atomic force micrograph (AFM) of a single CCG sheet. The SEMs of the nanocomposite (a) before, and (b) after $SOCl_2$ treatment indicate that the carbon nanotubes bundle up on top of the graphene layers. (c) SEMs show an increased overlap between graphene layers after (d) doping with $SOCl_2$. AFM images of CCG (e) before and (f) after treatment suggest that exposure to thionyl chloride can be detrimental to the overall fidelity of a graphene flake. This anionic dopant does not induce intercalation and folding, but rather causes rips and wrinkles.

Proposed mechanism of chloride anion doping

Scheme 1 illustrates a proposed reaction mechanism where thionyl chloride interacts in a nucleophilic fashion with a carboxylic acid. In the presence of thionyl chloride, a carbonyl oxygen can form a sulfite ester intermediate which readily reacts with nucleophiles, as it is a good leaving group. Upon formation of the acyl chloride, the displaced sulfite ion is unstable and decomposes into SO_2 and Cl^-. Analogous reactions with CCG and carbon nanotubes where the edges and basal planes are functionalized with hydroxyl and carboxylic functionalities explain how thionyl chloride modification takes place. In the case of pG, the edges are the preferred reaction sites and would likely chlorinate at terminating carbons.[23]

The effects of $SOCl_2$ on CNTs have been investigated, and it was found that the doping mechanism occurs predominantly *via* bonding of sulfur to the graphitic backbone, with very little C–Cl interactions.[7,9] This doping mechanism was therefore expected for pristine graphene, but that is not the case. We find that this proposed scheme applies to CCG and functionalized CNTs films. In the case of peeled graphene, chlorine anions formed in the vapour phase readily adsorb onto the surface and react with the delocalized π system halogenating preferentially along the edges, as they are the most energetically favorable locations.[23] Since chlorination of pristine graphene is possible with thionyl

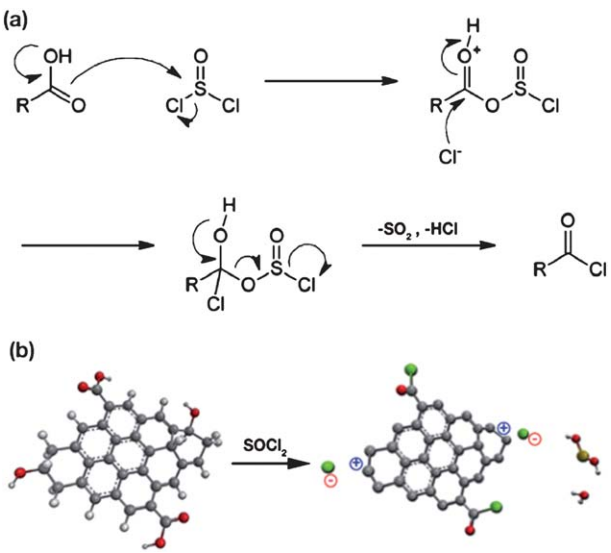

Scheme 1 (a): Proposed reaction mechanism in which thionyl chloride undergoes a nucleophilic interaction with a carboxylic acid releasing a chloride, which in turn can functionalize groups present on chemically converted graphenes and oxidized carbon nanotubes. R represents polyaromatic hydrocarbon species; (b) visualization of how chloride ions (green circles) are bonded to the carbons at the edge of a graphitic base.

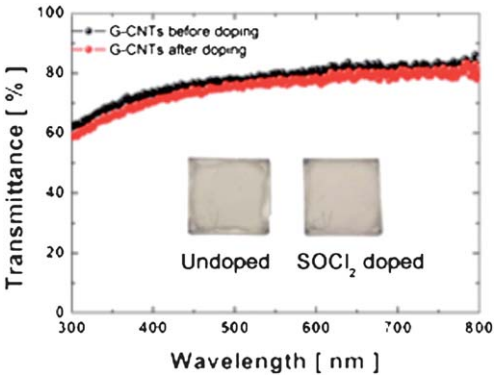

Fig. 4 Optical transmittance of thionyl chloride treated G–CNT films. Inset: photographic images of a G–CNT substrate before (left) and after doping (right) show essentially no change in transparency.

chloride, it is likely that other chlorinating agents will react in a similar fashion.

Optical transmission and electrical conductivity

Maintaining optical transmittance with high conductivity is vital for transparent conductor applications. Nitric acid doping of CNTs and CVD graphene shows no significant drop in transmittance while reducing the resistance by about 60%. [8] However, doping with bromine and iodine imparts a significant drop in transmittance after treatment. Doping with those halogens resulted in ~20% loss in transparency with comparable reductions in resistance. Optical transmittance measurements of G–CNT films across the UV-visible spectrum show that doping with $SOCl_2$ does not affect the transparency of G–CNT films, but it does enhance the electrical properties (Fig. 4). The inset images of a G–CNT substrate before (left) and after doping (right) are shown to visually verify that essentially no change in transparency or film quality has occurred.

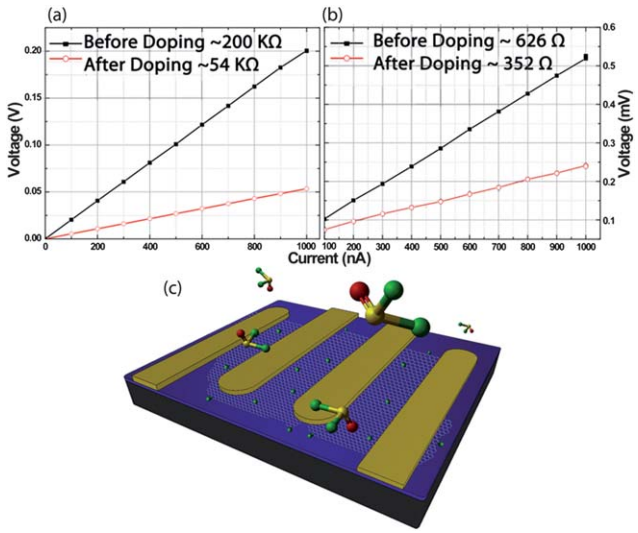

Fig. 5 Four-point probe measurements taken across single CCG and pG flakes of similar dimensions show a significant decrease in resistance after doping. (a) A single CCG flake shows an ~73% decrease in resistance while (b) mechanically exfoliated graphene shows an ~44% decrease in sheet resistance. (c) A computer generated illustration of a graphene sheet being decorated with chlorine along the edges and basal plane, which increases the number of positive charge carriers in the conjugated sp^2 network.

To further characterize the electronic properties of the different graphenes, flakes of CCG and pG were placed onto aligned substrates and gold electrodes were patterned using e-beam lithography. The resistance data were collected before and after exposure to $SOCl_2$ (Fig. 5a,b). As metals are susceptible to corrosion when exposed directly to thionyl chloride, *in vacuo* gate modulation measurements were not collected to observe the shift in the Dirac point from its origin. Nevertheless, we found appreciable resistance drops, and attribute them to the adsorbed chlorines along the basal plane of both graphenes, which ionically contribute holes to the conjugated sp^2 network. Additionally, the enhanced properties are believed to arise from C–Cl bonds resulting from newly formed charge-transfer complexes. Fig. 5c shows a computer generated illustration of a graphene sheet being decorated with chlorine along the edges and the basal plane, which increase the number of holes in the conjugated sp^2 network.

Conclusions

While the bonding in pristine graphene is just sp^2 carbon, chemically converted graphene contains residual oxygen moieties which can be readily functionalized for other applications. It was therefore assumed that pristine graphene would be less responsive to chlorination and more susceptible to sulfonation, as seen for other graphitic systems. However, based on the XPS, EDX and Raman spectra we conclude that vapour-phase thionyl chloride decomposes more readily and the resulting chlorine anions can effectively chlorinate oxygen containing graphene through a dehydration mechanism and the edges of peeled graphene through halogenation reactions. Additionally, chlorine anions adsorb onto the basal plane of graphene which also enhance the p-type behavior of the graphitic systems. Electrons residing on graphene are drawn towards the chlorine, which creates hole charge carriers in the graphitic systems and leads to a substantial decrease in resistance. Another reason for the increase in conductivity stems from morphological changes in the graphene thin films, which bring the sheets into closer proximity to each other. In addition to enhancing the electrical properties, we observe that the transparency of the G–CNT films is preserved. SEM and AFM images indicate that this vapour treatment can lead to wrinkles and induce aggregation of sheets and carbon nanotubes when they are in close proximity to each other. These results provide insights into the mechanism of functionalization of graphene and carbon nanotubes with vapour-phase ions and demonstrate a simple method to improve conductivity without sacrificing transparency of graphitic films.

Acknowledgements

The authors thank Minsheng Wang and Dr Li-Min Chen for assistance with collecting resistance and XPS data and the NSF IGERT Materials Creation Training Program (DGE-0114443) (KCC), the FENA FCRP Center at UCLA (RBK) and the Air Force Office of Scientific Research (AFOSR, fund

#FA9550-07-1-0264) (YY) for financial support. Instrumentation has been provided by the NanoPico Lab at the UCLA based California NanoSystems Institute.

References

1 K. S. Novoselov, A. K. Geim, S. V. Morozov, D. Jiang, Y. Zhang, S. V. Dubonos, I. V. Grigorieva and A. A. Firsov, *Science*, 2004, **306**, 666.
2 V. C. Tung, L.-M. Chen, M. J. Allen, J. K. Wassei, K. Nelson, R. B. Kaner and Y. Yang, *Nano Lett.*, 2009, **9**, 1949.
3 K. Lee, Z. Wu, Z. Chen, F. Ren, S. J. Pearton and A. G. Rinzler, *Nano Lett.*, 2004, **4**, 911.
4 Z. Wu, Z. Chen, X. Du, J. M. Logan, J. Sippel, M. Nikolou, K. Kamaras, J. R. Reynolds, D. B. Tanner, A. F. Hebard and A. G. Rinzler, *Science*, 2004, **305**, 1273.
5 A. D. Pasquier, H. E. Unalan, A. Kanwal, S. Miller and M. Chhowalla, *Appl. Phys. Lett.*, 2005, **87**, 203511.
6 J. K. Wassei and R. B. Kaner, *Mater. Today*, 2010, **13**, 52.
7 A. Kasry, M. A. Kuroda, G. J. Martyna, G. S. Tulevski and A. A. Bol, *ACS Nano*, 2010, **4**, 3839–3844.
8 S. Bae, H. Kim, Y. Lee, X. Xu, J.-S. Park, Y. Zheng, J. Balakrishnan, T. Lei, H. Ri Kim, Y. I. Song, Y.-J. Kim, K. S. Kim, B. Ozyilmaz, J.-H. Ahn, B. H. Hong and S. Iijima, *Nat. Nanotechnol.*, 2010, **5**, 574–578.
9 N. Jung, N. Kim, S. Jockusch, P. Kim and L. Brus, *Nano Lett.*, **9**, 4133–4137.
10 K. K. Kim, A. Reina, Y. Shi, H. Park, L.-J. Li, Y. H. Lee and J. Kong, *Nanotechnology*, 2010, **21**, 285205.
11 P. Blake, P. D. Brimicombe, R. R. Nair, T. J. Booth, D. Jiang, F. Schedin, L. A. Ponomarenko, S. V. Morozov, H. F. Gleeson, E. W. Hill, A. K. Geim and K. S. Novoselov, *Nano Lett.*, 2008, **8**, 1704–1708.
12 H.-Z. Geng, K. K. Kim, K. P. So, Y. S. Lee, Y. Chang and Y. H. Lee, *J. Am. Chem. Soc.*, 2007, **129**, 7758–7759.
13 M. A. Hamon, J. Chen, H. Hu, Y. Chen, M. E. Itkis, A. M. Rao, P. C. Eklund and R. C. Haddon, *Adv. Mater.*, 1999, **11**, 834.
14 U. Dettlaff-Weglikowska, V. Skakalova, R. Graupner, S. H. Jhang, B. H. Kim, H. J. Lee, L. Ley, Y. W. Park, S. Berber, D. Tomanek and S. Roth, *J. Am. Chem. Soc.*, 2005, **127**, 5125.
15 G. Eda, G. Fanchini and M. Chhowalla, *Nat. Nanotechnol.*, 2008, **5**, 270.
16 H.-J. Shin, S. M. Kim, S.-M. Yoon, A. Benayad, K. K. Kim, S. J. Kim, H. K. Park, J.-Y. Choi and Y. H. Lee, *J. Am. Chem.Soc.*, 2008, **130**, 2062.
17 V. C. Tung, M. J. Allen, Y. Yang and R. B. Kaner, *Nat. Nanotechnol.*, 2009, **4**, 25.
18 M. S. Dresselhaus, A. Jorio, M. Hofmann, G. Dresselhaus and R. Saito, *Nano Lett.*, 2010, **10**, 751.
19 A. C. Ferrari, *Solid State Commun.*, 2007, **143**, 47.
20 A. C. Ferrari, J. C. Meyer, V. Scardaci, C. Casiraghi, M. Lazzeri, F. Mauri, S. Piscanec, D. Jiang, K. S. Novoselov, S. Rothand and A. K. Geim, *Phys. Rev. Lett.*, 2006, **97**, 187401.
21 A. M. Rao, P. C. Eklund, S. Bandow, A. Thess and R. E. Smalley, *Nature*, 1997, **388**, 257.
22 M. J. Allen, M. Wang, S. A. V. Jannuzzi, Y. Yang, K. L. Wang and R. B. Kaner, *Chem. Commun.*, 2009, 6285.
23 X. Wang, X. Li, L. Zhang, Y. Yoon, P. K. Weber, H. Wang, J. Guo and H. Dai, *Science*, 2009, **324**, 5928.

